Convergence analysis of a partial differential algebraic system from coupling a semiconductor model to a circuit model

Michael Matthes *, Caren Tischendorf

University of Cologne, Institute of Mathematics, Germany

ABSTRACT

We are interested in circuit simulation including distributed semiconductor models. The circuit itself is modeled by the modified nodal analysis. The stationary drift diffusion equations are used to describe the semiconductors. The complete system is then a partial differential-algebraic system. We discretize it first in space with finite elements and the Scharfetter–Gummel discretization. The resulting semi-discrete system can be analyzed as a differential-algebraic equation with properly stated leading term. We present topological index one criteria. They coincide with previous results for the non-discretized partial differential-algebraic equation. For the time discretization we use standard BDF methods (implicit Gear formulas). Finally we derive a convergence estimate for the whole partial differential-algebraic system close to equilibrium.

© 2010 IMACS. Published by Elsevier B.V. All rights reserved.

1. Introduction

Modern circuit design has to deal with high frequencies combined with the miniaturization in chip technology. The common practice to replace semiconductor elements by equivalent circuits becomes more and more inefficient. Such equivalent circuits may contain more than 800 parameters for one transistor element. Hence it is worthwhile to use PDE models as the drift diffusion model (DD-model) [5]. These equations are coupled with a system of differential-algebraic equations coming from the modified nodal analysis (MNA) [10,4]. The coupling is given by the coupling current on the one hand and by the voltage that is applied to the semiconductor on the other hand. The latter contributes to the DD-model as a boundary condition. This is briefly described in the second section. In contrast to [21] we investigate the coupling of the circuit with the *stationary* DD-model. It allows us to use convergence estimates given in [12].

In order to solve the resulting system numerically, it is first discretized in space and then in time. The space discretization is done with finite elements and the Scharfetter–Gummel discretization [18] which is briefly described in Section 3. The space discretized or semi-discrete system forms a differential-algebraic equation with a properly stated leading term and can be investigated in terms of the tractability index [13], see Section 4. Section 5 is devoted to the time discretization by backward differentiation formulas (BDF-method).

Finally, in Section 6, we present a convergence estimate for the numerical solution of the complete system relying on estimates by MARKOWICH in [12] for the DD-model and by HIGUERAS and MÄRZ in [9] for the BDF-method.

---

* Corresponding author.
E-mail addresses: mmatthes@math.uni-koeln.de (M. Matthes), tischendorf@math.uni-koeln.de (C. Tischendorf).

2. Modeling

In this part we review quite briefly the Modified Nodal Analysis, the stationary drift diffusion model and the coupling equations.

We consider an electrical circuit which is represented as a graph with n nodes and b branches. Resistors, capacitors, inductors and independent voltage and current sources are located on the branches. From the MNA we end up with the following set of equations, [19,22]:

$$A_C \frac{dq_C(A_C^T e, t)}{dt} + A_R g(A_R^T e, t) + A_L j_L + A_V j_V + A_I i_s(t) = 0, \tag{1}$$

$$\frac{d\phi(j_L, t)}{dt} - A_L^T e = 0, \tag{2}$$

$$A_V^T e - v_s(t) = 0. \tag{3}$$

Here the unknowns are the node potentials $e(t) : \mathbb{R} \to \mathbb{R}^{n-1}$ excepting the mass node, the currents through inductors $j_L(t) : \mathbb{R} \to \mathbb{R}^{b_L}$ and the currents through voltage sources $j_V(t) : \mathbb{R} \to \mathbb{R}^{b_V}$. The matrices $A_X \in \mathbb{R}^{(n-1) \times b_X}$ for $X \in \{R, C, L, V, I\}$ are the element-related (reduced) incidence matrices having entries from $\{-1, 0, 1\}$. The input functions $i_s(t)$ and $v_s(t)$ are related to the independent current and voltage sources respectively while the functions $q_C(u, t)$, $g(u, t)$ and $\phi(j, t)$ are associated to the physical relations given for charge, conductance and flux.

As a mathematical model for the semiconductor behavior we rely on the scaled stationary DD-model. It is extensively described in [12,20,22]. We formulate it here in just one spatial dimension, where $\overline{\Omega} = [0, l] \subset \mathbb{R}$ is the range of the device including its contacts at $x = 0$ and $x = l$. The time is represented by $t \in \mathcal{I} := [t_0, T]$. By $'$ we denote the partial derivative with respect to the space variable x. We have the Poisson equation

$$\lambda^2 \psi''(x, t) = n(x, t) - p(x, t) - C(x) \quad \text{for } (x, t) \in \Omega \times \mathcal{I}$$

which describes the electrostatic potential ψ in relation to the density of electrons n, the density of holes p and the doping profile C. The scalar λ is the scaled Debye length [11]. Furthermore we have the continuity equations

$$J_n'(x, t) = R,$$
$$J_p'(x, t) = -R$$

and the current density equations

$$J_n(x, t) = \mu_n(x)\big(n'(x, t) - n(x, t)\psi'(x, t)\big),$$
$$J_p(x, t) = -\mu_p(x)\big(p'(x, t) + p(x, t)\psi'(x, t)\big).$$

Here J_n and J_p are the electron current density and the hole current density resp., μ_n and μ_p are the mobilities and R is the recombination–generation rate. In the following we will restrict ourselves to the Shockley–Read–Hall model for the recombination–generation rate

$$R = R_{SRH} = \frac{np - \delta^4}{\tau_p(n + \delta^2) + \tau_n(p + \delta^2)}$$

where τ_n and τ_p are the average lifetimes of the electrons and holes and δ^2 is the scaled intrinsic carrier density concentration, cf. [12]. Furthermore there are the following boundary conditions on $\partial\Omega \times \mathcal{I}$:

$$\psi(x, t) = \frac{1}{U_T}\big(\psi_{ap}(x, t) + \psi_{bi}(x)\big), \tag{4}$$

$$n(x, t) = \frac{1}{2}\big(\sqrt{C^2(x) + 4\delta^4} + C(x)\big), \tag{5}$$

$$p(x, t) = \frac{1}{2}\big(\sqrt{C^2(x) + 4\delta^4} - C(x)\big) \tag{6}$$

where U_T is the thermal voltage and ψ_{bi} is the built-in potential given by

$$\psi_{bi}(x) := U_T \ln\left(\frac{C(x) + \sqrt{C^2(x) + 4\delta^4}}{2\delta^2}\right).$$

ψ_{ap} is the applied potential which we will address later in detail.

In order to couple the MNA with the scaled stationary DD-model we have to scale the MNA-equations, introduce a coupling current and discuss the applied potential. The relevant scaling of the MNA-equations was already done in [21] and will not be discussed here any further. The resulting equations are the same as (1)–(3) if we identify the scaled variables

with the same symbols used for the unscaled variables. For the coupling current we again refer to [21], we just neglect the drift current which is not present in the stationary model. As we have only one spatial dimension the current through the contacts at $x = 0, l$ is given by

$$j_S(x, t) = \alpha \big(J_n(x, t) + J_p(x, t) \big),$$

α being a scaling parameter taking also into account the area of the contacts. This equations originates from a boundary integral in the multidimensional case which reduces to a pointwise equation in the one-dimensional case, cf. e.g. [12,22,14, 21]. Since the DD-model is charge conserving [22], we can express them by each other: $j_S(0, t) = -j_S(l, t)$. Hence we can define $x = l$ to be the reference contact. For the applied potential we set

$$\psi_{ap}|_{x=0} := e_i - e_j,$$
$$\psi_{ap}|_{x=l} := 0$$

if the semiconductor element lies between the nodes i and j of the network and j is connected to the reference contact. To write this neatly in terms of incidence matrices we define $A_S = (a_{ik}) \in \mathbb{R}^{(n-1) \times b_S}$ as follows:

$$a_{ik} := \begin{cases} -1, & \text{if the reference contact of semiconductor } k \text{ lies at node } i, \\ 1, & \text{if the non-reference contact of semiconductor } k \text{ lies at node } i, \\ 0, & \text{else.} \end{cases}$$

Here b_S is the number of semiconductor elements in the circuit. With $j_S = (j_{S,1}, \ldots, j_{S,b_S})^T$ we denote the vector of currents which are at the non-reference contact. Including this in the first MNA-equation (1) yields

$$A_C \frac{dq_C(A_C^T e, t)}{dt} + A_R g(A_R^T e, t) + A_L j_L + A_V j_V + A_I i_s(t) + A_S j_S = 0$$

and also the applied potential can be expressed nicely as:

$$\psi_{ap}|_{x=0} = A_S^T e.$$

For the following analysis we restrict ourselves to only one semiconductor present in the circuit. It can be easily extended to the case of several semiconductor elements. So j_S is a scalar time dependent function. We get the system

$$A_C \frac{dq_C(A_C^T e, t)}{dt} + A_R g(A_R^T e, t) + A_L j_L + A_V j_V + A_I i_s(t) + A_S j_S = 0, \tag{7a}$$

$$\frac{d\phi(j_L, t)}{dt} - A_L^T e = 0, \tag{7b}$$

$$A_V^T e - v_s(t) = 0, \tag{7c}$$

$$j_S - \alpha \big(J_n(0, t) + J_p(0, t) \big) = 0, \tag{7d}$$

$$-\lambda^2 \psi'' - (n - p - C) = 0, \tag{7e}$$

$$\big(\mu_n (n' - n\psi') \big)' - R = 0, \tag{7f}$$

$$\big(-\mu_p (p' + p\psi') \big)' + R = 0. \tag{7g}$$

3. Space discretization

The first step is now to discretize the system above in space with finite elements, for example. For simplicity we split the space interval $\overline{\Omega} = [0, l]$ into equally-spaced subintervals $T_j := [x_j, x_{j+1}]$ of length h for $j = 1, \ldots, m - 1$ and $x_1 = 0$ and $x_m = l$. On this simple grid we define the finite-dimensional vector space $V_h \subseteq H^1(\Omega)$ as the space of all functions which are linear on every T_j and continuous on $\overline{\Omega}$. Additionally we define $V_{h,0} := \{f \in V_h \mid f(0) = f(l) = 0\} \subseteq H_0^1(\Omega)$. The standard basis functions φ_l for $l = 1, \ldots, m$ for these spaces are defined by

$$\varphi_l(x_i) := \begin{cases} 1, & i = l \\ 0, & i \neq l \end{cases} \quad \forall i = 1, \ldots, m.$$

Furthermore we discretize the right hand side of the Poisson equation with the trapezoidal rule and we can write down the Galerkin equations:

$$T\Psi - \frac{h^2}{\lambda^2}(C - N + P) - \Psi_0 \big(A_S^T e \big) = 0 \tag{8}$$

where

$$T := \begin{pmatrix} 2 & -1 & & & \\ -1 & \ddots & \ddots & & \\ & \ddots & \ddots & -1 \\ & & -1 & 2 \end{pmatrix}, \qquad \Psi_0(A_S^T e) := \begin{pmatrix} \psi_D(0) \\ 0 \\ \vdots \\ 0 \\ \psi_D(l) \end{pmatrix} = \frac{1}{U_T} \begin{pmatrix} \psi_{bi}(0) + A_S^T e \\ 0 \\ \vdots \\ 0 \\ \psi_{bi}(l) \end{pmatrix}$$

and the vectors of node values in $\mathbb{R}^{m-2}$

$$\Psi := \begin{pmatrix} \psi_2 \\ \vdots \\ \psi_{m-1} \end{pmatrix}, \qquad N := \begin{pmatrix} n_2 \\ \vdots \\ n_{m-1} \end{pmatrix}, \qquad P := \begin{pmatrix} p_2 \\ \vdots \\ p_{m-1} \end{pmatrix}, \qquad C := \begin{pmatrix} C(x_2) \\ \vdots \\ C(x_{m-1}) \end{pmatrix}.$$

For the continuity equations we rely on the so called Scharfetter–Gummel discretization [18]. This discretization is often used for semiconductor device simulation since the current densities do not have as steep gradients as n and p have. Here it is assumed that the current densities J_n and J_p are constant on the subintervals T_j. Following this idea a discretization formula for $J_{n,h}^j \approx J_n|_{T_j}$ for $j = 1, \ldots, m-1$ can be derived:

$$J_{n,h}^j = \mu_{n,h}^j \left[f(z_j) \left(\frac{e^{z_j} + 1}{2} \right) \left(\frac{n_{j+1} - n_j}{h} \right) - \left(\frac{n_j + n_{j+1}}{2} \right) \left(\frac{z_j}{h} \right) \right] \tag{9}$$

where $z_j = \psi_{j+1} - \psi_j$, $\mu_{n,h}^j = \mu_n(x_j + h/2)$ and $f(z)$ is given by:

$$f(z) := \begin{cases} \frac{z}{e^z - 1}, & z \neq 0, \\ 1, & z = 0. \end{cases}$$

An analogous formula for $J_{p,h}^j$ applies. For more detailed information on how this discretization is done we refer to [14, 12]. After using the trapezoidal rule for the recombination–generation rate we get the discretized version of the continuity equations:

$$-\frac{1}{h^2} g_1(A_S^T e, \Psi, N) + R(N, P) = 0, \tag{10}$$

$$\frac{1}{h^2} g_2(A_S^T e, \Psi, P) + R(N, P) = 0 \tag{11}$$

where g_1 and g_2 are nonlinear differentiable vector valued functions of dimension $m - 2$. We can write Eqs. (8), (10) and (11) into a nonlinear coupled system of algebraic equations for the variables Ψ, N and P:

$$G_{DD}(A_S^T e; \Psi, N, P) := \begin{pmatrix} T\Psi - \frac{h^2}{\lambda^2}(C - N + P) - \Psi_0(A_S^T e) \\ -\frac{1}{h^2} g_1(A_S^T e, \Psi, N) + R(N, P) \\ \frac{1}{h^2} g_2(A_S^T e, \Psi, P) + R(N, P) \end{pmatrix} = 0.$$

Assumption 3.1 (*Regularity of G'_{DD}*). The matrix $G'_{DD} := (G_{DD})'_{(\Psi, N, P)}(A_S^T e; \Psi, N, P)$ is non-singular if the applied voltage $A_S^T e$ is sufficiently small.

This assumption is motivated by the fact that MARKOWICH states the unique solvability of the discretized DD-system close to equilibrium, cf. [12, p. 151]. Furthermore it is shown there that the continuous DD-operator has a bounded inverse for small applied voltages.

Still the space discretization of the coupling current needs to be done because it depends on ψ, n and p even it does not explicitly depend on the space variable x. By using (9) we can replace Eq. (7d) by

$$j_{S,h} - j_{S,h}^{discr}(A_S^T e, \Psi, N, P) = 0$$

where $j_{S,h}^{discr}$ is a nonlinear differentiable scalar function. This is investigated more in detail in [14,12]. Finally the space discretized system looks like

$$A_C \frac{dq_C(A_C^T e, t)}{dt} + A_R g(A_R^T e, t) + A_L j_L + A_V j_V + A_I i_s(t) + A_S j_{S,h} = 0, \tag{12a}$$

$$\frac{d\phi(j_L, t)}{dt} - A_L^T e = 0, \tag{12b}$$

$$A_V^T e - v_s(t) = 0, \tag{12c}$$

$$j_{S,h} - j_{S,h}^{discr}\left(A_S^T e, \Psi, N, P\right) = 0, \tag{12d}$$

$$T\Psi - \frac{h^2}{\lambda^2}(C - N + P) - \Psi_0\left(A_S^T e\right) = 0, \tag{12e}$$

$$-\frac{1}{h^2}g_1\left(A_S^T e, \Psi, N\right) + R(N, P) = 0, \tag{12f}$$

$$\frac{1}{h^2}g_2\left(A_S^T e, \Psi, P\right) + R(N, P) = 0 \tag{12g}$$

for the time dependent variables e, j_L, j_V, $j_{S,h}$, Ψ, N and P.

4. Analysis of the space discretized system

In this section we analyze the space discretized system in terms of proper formulated differential-algebraic equations and the tractability index. We recall DAEs of the form (cf. [13])

$$A\frac{\mathrm{d}}{\mathrm{d}t}d\left(y(t), t\right) + b\left(y(t), t\right) = 0, \quad t \in \mathcal{I} \subseteq \mathbb{R} \tag{13}$$

with $A \in \mathbb{R}^{m \times n}$ and where d and b have continuous partial derivatives

$$D(y, t) := \frac{\partial}{\partial y}d(y, t) \quad \text{and} \quad B(y, t) := \frac{\partial}{\partial y}b(y, t).$$

We can write the system (12) in this form by setting

$$A = \begin{pmatrix} A_C & 0 \\ 0 & I \\ 0 & 0 \\ 0 & 0 \\ 0 & 0 \\ 0 & 0 \\ 0 & 0 \end{pmatrix}, \qquad d(y, t) = \begin{pmatrix} A_C^+ A_C q_C(A_C^T e, t) \\ \phi(j_L, t) \end{pmatrix}, \tag{14}$$

$$b(y, t) = \begin{pmatrix} A_R g(A_R^T e, t) + A_L j_L + A_V j_V + A_I i_s(t) + A_S j_{S,h} \\ -A_L^T e \\ A_V^T e - v_s(t) \\ j_{S,h} - j_{S,h}^{discr}(A_S^T e, \Psi, N, P) \\ T\Psi - \frac{h^2}{\lambda^2}(C - N + P) - \Psi_0(A_S^T e) \\ -\frac{1}{h^2}g_1(A_S^T e, \Psi, N) + R(N, P) \\ \frac{1}{h^2}g_2(A_S^T e, \Psi, P) + R(N, P) \end{pmatrix} \tag{15}$$

for

$$y(t) = \left(e(t), j_L(t), j_V(t), j_{S,h}(t), \Psi(t), N(t), P(t)\right)^T \in \mathbb{R}^{n-1+b_L+b_V+1+3(m-2)}.$$

A_C^+ is the Moore–Penrose inverse of A_C [17], hence in particular $A_C = A_C A_C^+ A_C$. It can be easily seen that the space discretized system (12) written as above has a properly stated leading term, cf. [13,14].

In order to identify if this system has tractability index one [13] we recall some basic assumptions we make for the circuit, cf. [21]:

Assumption 4.1 *(Basic assumptions on the circuit).*

- The input functions $i_s(t)$ and $v_s(t)$ for the independent current and voltage sources respectively are continuous.
- The functions $q_C(u, t)$, $g(u, t)$ and $\phi(j, t)$ are continuously differentiable and have positive definite Jacobians

$$C(u, t) := \frac{\partial q_C(u, t)}{\partial u},$$

$$G(u, t) := \frac{\partial g(u, t)}{\partial u},$$

$$L(j,t) := \frac{\partial \phi(j,t)}{\partial j}$$

for all u, j, t.

- There exist no loops of voltage sources or cutsets of current sources in the network.

With the second assumption we restrict ourselves here to passive elements and the third assumption is necessary in order to avoid short circuits. Furthermore we call a cutset an LI-cutset if it only consists of inductivities and current sources. A CV-loop is a loop which only contains capacitances and voltage sources. We call a path a capacitive path if it only consists of capacitances. BODESTEDT proved in [3] that the semiconductor nodes are connected by a capacitive path if and only if $A_S^T Q_C = 0$ for a projector Q_C on $\ker A_C^T$.

Theorem 4.2 (Index 1 of the space discretized system). *Let Assumptions* 3.1 *and* 4.1 *be fulfilled. The semiconductor nodes should be connected by a capacitive path and the applied potential* $A_S^T e$ *should be sufficiently small. Then the space discretized system* (12) *in its proper formulation via* (14) *and* (15) *has tractability index one if the network contains neither LI-cutsets nor CV-loops with at least one voltage source.*

Proof. It is quite straightforward to see that $G_0 = AD$ is singular because

$$\ker AD = \ker A_C^T \times \{0\}^{b_L} \times \mathbb{R}^{b_V} \times \mathbb{R} \times \left(\mathbb{R}^{m-2}\right)^3 \tag{16}$$

and our network contains a semiconductor. To prove the non-singularity of $G_1 = G_0 + BQ$ with Q being a projector onto $N_0 = \ker G_0$ we can take

$$Q = \begin{pmatrix} Q_C & 0 & 0 \\ 0 & 0 & 0 \\ 0 & 0 & I_{b_V + 1 + 3(m-2)} \end{pmatrix}.$$

With (16) it follows that Q is a projector onto N_0, if Q_C is a projector onto $\ker A_C^T$. We compute

$$G_1 = AD + BQ$$

$$= \left(\begin{array}{ccc|c|ccc} A_C C(\cdot) A_C^T + A_R G(\cdot) A_R^T Q_C & 0 & A_V & A_S & 0 & 0 & 0 \\ -A_L^T Q_C & L(\cdot) & 0 & 0 & 0 & 0 & 0 \\ A_V^T Q_C & 0 & 0 & 0 & 0 & 0 & 0 \\ \hline -\frac{\partial j_{S,h}^{discr}}{\partial e} Q_C & 0 & 0 & 1 & -\frac{\partial j_{S,h}^{discr}}{\partial \Psi} & -\frac{\partial j_{S,h}^{discr}}{\partial N} & -\frac{\partial j_{S,h}^{discr}}{\partial P} \\ -\frac{\partial \Psi_0}{\partial e} Q_C & 0 & 0 & 0 & T & \frac{h^2}{\lambda^2} I_{m-2} & -\frac{h^2}{\lambda^2} I_{m-2} \\ -\frac{1}{h^2} \frac{\partial g_1}{\partial e} Q_C & 0 & 0 & 0 & -\frac{1}{h^2}\frac{\partial g_1}{\partial \Psi} & -\frac{1}{h^2}\frac{\partial g_1}{\partial N} + \frac{\partial R}{\partial N} & \frac{\partial R}{\partial P} \\ \frac{1}{h^2} \frac{\partial g_2}{\partial e} Q_C & 0 & 0 & 0 & \frac{1}{h^2}\frac{\partial g_1}{\partial \Psi} & \frac{\partial R}{\partial N} & \frac{1}{h^2}\frac{\partial g_1}{\partial P} + \frac{\partial R}{\partial P} \end{array} \right)$$

$$= \left(\begin{array}{c|c|c} & A_S & \\ G_1^{MNA} & & \\ \hline -\partial_1 j_{S,h}^{discr} A_S^T Q_C & 1 & * \\ -\partial_1 \Psi_0 A_S^T Q_C & & \\ -\frac{1}{h^2} \partial_1 g_1 A_S^T Q_C & & \\ \frac{1}{h^2} \partial_1 g_2 A_S^T Q_C & & G_{DD}'(A_S^T e; \Psi, N, P) \end{array} \right).$$

With ∂_1 we denoted the derivative with respect to the first component. Since the semiconductors are connected by a capacitive path we have $A_S^T Q_C = 0$ and so the entries in the lower left block all vanish. Under the assumptions above it was shown in [22] that G_1^{MNA} is non-singular. Because of Assumption 3.1 the matrix G_{DD}' is non-singular and so is G_1. □

We have the same index result as for the continuous system in [3]. The fact that we assume the semiconductor nodes to be connected by a capacitive path is crucial there as well. It is also needed for proving the existence of a solution of the coupled continuous problem, cf. [1]. This requirement might look unnatural but it actually makes physically sense when using the stationary DD-model. Having time dependent boundary conditions the electrical field $E = -\psi'$ varies over time. So charge carriers are redistributed on either side of the pn-junctions which creates an additional current over the contacts. To compensate this dynamical (or capacitive) behavior it is physically reasonable to put a small capacitance in parallel to the semiconductor, cf. [3]. Coupling the nonstationary DD-model to a circuit such a parallel capacitance is not needed, cf. [21,3].

5. Time discretization

We discretize the DAE (12) above or equivalently (13) in time with the K-step backward differentiation formula (BDF method), cf. [6]. In circuit simulation the BDF method is well established from a practical point of view in comparison to e.g. Runge–Kutta methods (RK methods). Since highly dimensional systems have to be solved function evaluations are expensive. So in circuit simulation the computational cost is prohibitive for the (fully implicit) RK-methods which can be used with DAEs. More discussion on that can be found in [23]. Hence we will investigate the BDF-method in the following for solving the space discretized system numerically. We restrict ourselves to $K \leqslant 6$ because otherwise the BDF are not stable anymore. To compute an approximation y_n to $y(t_n)$ we need K former values $y_{n-K}, \ldots, y_{n-1}$. We work with constant stepsize $\tau = t_n - t_{n-1}$. We have to solve the following system, compare e.g. [23]:

$$A[d]'_n + b(y_n, t_n) = 0, \tag{17a}$$

$$[d]'_n = \frac{1}{\tau} \sum_{j=0}^{K} \alpha_j d(y_{n-j}, t_{n-j}) \tag{17b}$$

where the α_j, $j = 0, \ldots, K$ are the well-known BDF coefficients. In [9] a convergence result was shown for the K-step BDF for a system of the form

$$A \frac{\mathrm{d}}{\mathrm{d}t} \big(D(t) y(t) \big) + b \big(y(t), t \big) = 0.$$

This can be easily transferred to our situation here. This was done extensively in [9,14] and we have the following result.

Theorem 5.1. *For the solution $y_*(t)$ of the DAE (13) with tractability index one $d(y_*(\cdot), \cdot) \in C^{K+1}$ and $d(y_l, t_l) - d(y_*(t_l), t_l) = \mathcal{O}(\tau^K)$, $l = 0, \ldots, K-1$ should be satisfied. Then the K-step BDF as described above in (17) are convergent with order K, i.e.*

$$\exists C > 0: \quad \big\| y_n - y_*(t_n) \big\|_\infty \leqslant C \tau^K.$$

This result is still true for variable stepsizes τ_n if certain bounds on the stepsize ratios apply, cf. [9]. For convenience later we extract here the assumptions:

Assumption 5.2. For the solution $y_*(t)$ of the DAE (13) holds $d(y_*(\cdot), \cdot) \in C^{K+1}$ and $d(y_l, t_l) - d(y_*(t_l), t_l) = \mathcal{O}(\tau^K)$, $l = 0, \ldots, K-1$.

Having a look at Eq. (14) we see that the smoothness condition of Assumption 5.2 implies that for solving the coupled system the functions q_C and ϕ have to be smooth enough. In the common linear case no problems arise here while for nonlinear functions for charge and flux there can be restrictions on the order K.

6. Convergence analysis

We expect a solution

$$w(t) := \big(e(t), j_L(t), j_V(t), j_S(t), \psi(\cdot, t), n(\cdot, t), p(\cdot, t) \big)^T$$

of the system (7) to be in the space

$$H := \mathbb{R}^{n-1+b_L+b_V+1} \times \big(H^1(\Omega) \big)^3$$

with the norm

$$\begin{aligned} \big\| w(t) \big\|_H &:= \big\| e(t) \big\|_\infty + \big\| j_L(t) \big\|_\infty + \big\| j_V(t) \big\|_\infty + \big| j_S(t) \big| \\ &\quad + \big\| \psi(\cdot, t) \big\|_{1,2,\Omega} + \big\| n(\cdot, t) \big\|_{2,\Omega} + \big\| p(\cdot, t) \big\|_{2,\Omega}. \end{aligned}$$

Here we used the standard L_2- resp. H^1-norms:

$$\| f \|_{2,\Omega}^2 = \int_\Omega f(x)^2 \, dx, \qquad \| f \|_{1,2,\Omega}^2 = \int_\Omega f(x)^2 \, dx + \int_\Omega f'(x)^2 \, dx.$$

Assumption 6.1. Let the requirements of Theorem 4.2 be fulfilled. Furthermore let an a-priori estimate for the network variables of the form

$$\big\| \big(e(t), j_L(t), j_V(t) \big)^T \big\|_\infty \leqslant K, \quad \forall t \in \mathcal{I} \tag{18}$$

of a solution w to (7) for a sufficiently small $K > 0$ be given.

The only existence result of a solution to the coupled system (7) with Shockley–Read–Hall recombination–generation term can be found in [1]. It is also mentioned there that close to thermal equilibrium a unique solution is expected. Furthermore the a-priori estimate (18) is given in [1]. This factor K only depends on the initial values e_0, $j_{L,0}$, $j_{V,0}$ and on the input functions i_s and v_s. Choosing these appropriately it can be ensured that K is sufficiently small and thus the applied potential $A_S^T e$ is small as well.

After space discretization of (7) we arrive at (12). The solution of (12) at $t \in \mathcal{I}$ we denote by

$$w_h(t) = \left(e(t), j_L(t), j_V(t), j_{S,h}(t), \psi_h(\cdot, t), n_h(\cdot, t), p_h(\cdot, t) \right)^T \in H_h$$

with

$$H_h := \mathbb{R}^{n-1+b_L+b_V+1} \times V_h^3 \subseteq H$$

or by

$$y(t) = \left(e(t), j_L(t), j_V(t), j_{S,h}(t), \Psi(t), N(t), P(t) \right)^T \in \mathbb{R}^r$$

where $r := n - 1 + b_L + b_V + 1 + 3(m - 2)$. These two expressions of a solution of the space discretized system are in the following sense equivalent. We can see that by defining the interpolation mapping

$$\vartheta : \mathbb{R}^r \to H_h$$

with

$$\vartheta : (e, j_L, j_V, j_{S,h}, \Psi, N, P)^T \mapsto \left(e, j_L, j_V, j_{S,h}, \sum_{i=1}^m \psi_i \varphi_i, \sum_{i=1}^m n_i \varphi_i, \sum_{i=1}^m p_i \varphi_i \right)^T.$$

The φ_i are the basis functions of V_h, ψ_i, n_i and p_i for $i = 2, \ldots, m-1$ are the entries of Ψ, N, P and the boundary data for $i = 1, m$ is given as described in (4)–(6).

Corollary 6.2. *The mapping ϑ is injective and $\vartheta(y(t)) = w_h(t)$ for all $t \in \mathcal{I}$.*

Finally after time discretization we arrive at a solution y_l of (17a), (17b) at $t = t_l$:

$$y_l = (e_l, j_{L,l}, j_{V,l}, j_{S,h,l}, \Psi_l, N_l, P_l)^T \in \mathbb{R}^r$$

where

$$\Psi_l = \begin{pmatrix} \psi_{2,l} \\ \vdots \\ \psi_{m-1,l} \end{pmatrix}, \qquad N_l = \begin{pmatrix} n_{2,l} \\ \vdots \\ n_{m-1,l} \end{pmatrix}, \qquad P_l = \begin{pmatrix} p_{2,l} \\ \vdots \\ p_{m-1,l} \end{pmatrix}.$$

In order to compare the exact solution $w(t_l)$ with the approximation y_l we have to do it in the same space. We want to do that in H. Therefore we use the interpolation mapping ϑ and get

$$\left\| w(t_l) - \vartheta(y_l) \right\|_H \leqslant \left\| w(t_l) - w_h(t_l) \right\|_H + \left\| w_h(t_l) - \vartheta(y_l) \right\|_H \tag{19}$$

because $\vartheta(y_l) \in H_h \subseteq H$. As a consequence we can split the whole estimate in two parts, one for the space discretization and the other one for the time discretization.

If we look at the space discretization first, i.e. at the first term of (19) we see that

$$\left\| w(t) - w_h(t) \right\|_H = \left| j_S(t) - j_{S,h}(t) \right| + \left\| \psi(\cdot, t) - \psi_h(\cdot, t) \right\|_{1,2,\Omega}$$
$$+ \left\| n(\cdot, t) - n_h(\cdot, t) \right\|_{2,\Omega} + \left\| p(\cdot, t) - p_h(\cdot, t) \right\|_{2,\Omega}$$

since the components e, j_L and j_V of w do not depend on the space variable x. This means we can apply estimates from the DD-model here which were already presented by MARKOWICH in [12] and to some extent by MOCK in [16]: For the electrostatic potential holds

$$\| \psi - \psi_h \|_{1,2,\Omega}^\lambda = \mathcal{O}(h) \tag{20}$$

and

$$\| \psi - \psi_h \|_{2,\Omega} = \mathcal{O}(h^2). \tag{21}$$

With $\| \cdot \|_{1,2,\Omega}^{\lambda}$ we denote the weighted H^1-norm for $f \in H^1(\Omega)$:

$$\|f\|_{1,2,\Omega}^{\lambda} := \left(\|f\|_{2,\Omega}^2 + \lambda^2 \|f'\|_{2,\Omega}^2 \right)^{\frac{1}{2}}.$$

It can be easily seen that this norm is equivalent to the usual H^1-norm for fixed λ. Hence we also have

$$\|\psi - \psi_h\|_{1,2,\Omega} = \mathcal{O}(h). \tag{22}$$

Furthermore we have for the carrier densities

$$\|n - n_h\|_{2,\Omega} + \|p - p_h\|_{2,\Omega} = \mathcal{O}\left(h^2 \ln \frac{1}{h} \right) \tag{23}$$

and for the coupling current

$$|j_S - j_{S,h}| = \mathcal{O}\left(h^2 \ln \frac{1}{h} \right). \tag{24}$$

We remark that quadratic convergence is better than the convergence rate from (23) and (24) for $h \leqslant \exp^{-1}$. The assumptions which are necessary to show these results can be found in [12] (Chapters 3 and 5) and to some extent elaborated in [14]. They contain non-singularity and boundedness of certain operators. From the numerical point of view an important requirement is the assumption that all fast varying quantities have to be resolved well by the mesh. This means the stepsize h needs to be sufficiently small to guarantee the estimates above. Keeping this in mind we do not want to dwell on the precise requirements any further and so we simply assume

Assumption 6.3 *(Estimates for the space discretized system).* The estimates (21), (22), (23) and (24) are valid for sufficiently small stepsizes h.

The estimates above are valid for the DD-model itself but here we consider the coupled scenario. Since the boundary data changes in time we have these estimates for every timestep but with a different constant. We conclude that there exists a time dependent factor $c(A_S^T e) > 0$ such that

$$|j_S - j_{S,h}| + \|\psi - \psi_h\|_{1,2,\Omega} + \|n - n_h\|_{2,\Omega} + \|p - p_h\|_{2,\Omega} \leqslant c\left(A_S^T e\right) \left(h + h^2 \ln \frac{1}{h} \right).$$

We will assume in the following:

Assumption 6.4 *(Boundedness of $c(A_S^T e)$).* The factor $c(A_S^T e) > 0$ is bounded for bounded potential differences $A_S^T e(t)$, $t \in \mathcal{I}$, i.e.

$$\exists M > 0: \quad c\left(A_S^T e\right) \leqslant M \ \forall t \in \mathcal{I}$$

and this M is independent of t.

In order to prove this statement properly one has to go through all the proofs of (22)–(24) in [12]. It is still motivated by Theorem 4.4 in [3]. There it is shown that the linearized operator of the complete coupled system (7) has a bounded inverse near equilibrium. The fact that the linearized stationary DD-operator has a bounded inverse was already proven in [12] and is the starting point for proving the estimates (22)–(24).

Since we have the a-priori estimate (18) for the network variables we can guarantee the boundedness of $A_S^T e$ with Assumption 6.1. We conclude

Theorem 6.5 *(Estimate for the space discretization).* *Assumptions* 6.3, 3.1, 4.1, 6.1 *and* 6.4 *are valid. The semiconductor nodes are connected by a capacitive path and the network contains neither LI-cutsets nor CV-loops with at least one voltage source. If $A_S^T e$ is sufficiently small there exists an $M > 0$ such that*

$$\left\| w(t) - w_h(t) \right\|_H \leqslant M \left(h + h^2 \ln \frac{1}{h} \right)$$

for small stepsizes h and all $t \in \mathcal{I}$.

Proof. Because of the assumptions the original system is uniquely solvable and the space discretized system has tractability index one with Theorem 4.2. With Assumption 6.4 we get the estimate above. $\quad \square$

Now we may have a look at the second term of (19). In order to apply the estimate from Theorem 5.1 we need the following lemma:

Lemma 6.6. *Let $f \in V_h \subseteq H^1(\Omega)$ and $F = (f_2, \ldots, f_{m-1})^T$ be the vector of the inner grid values with $f_i := f(x_i)$ for $i = 1, \ldots, m$. Then*

$$\|f\|_{2,\Omega} \leqslant \sqrt{|\Omega|} \max\{|f_1|, |f_m|, \|F\|_\infty\}$$

and

$$\|f'\|_{2,\Omega} \leqslant \frac{2}{h} \sqrt{|\Omega|} \max\{|f_1|, |f_m|, \|F\|_\infty\}.$$

hold. Hereby we denoted the weak derivative of f by f'.

Proof. Since $f \in V_h$ the function f takes its maximum at the grid points. Hence we have

$$\begin{aligned}
\|f\|_{2,\Omega} &\leqslant \left(|\Omega| \max_{x \in \Omega} |f(x)|^2\right)^{\frac{1}{2}} \\
&= \sqrt{|\Omega|} \max_{x \in \Omega} |f(x)| \\
&= \sqrt{|\Omega|} \max\{|f_1|, |f_m|, \|F\|_\infty\}
\end{aligned}$$

and

$$\begin{aligned}
\|f'\|_{2,\Omega} &= \left(\sum_{j=1}^{m-1} \int_{T_j} |f'(x)|^2 \, dx\right)^{\frac{1}{2}} \\
&= \left(\sum_{j=1}^{m-1} \int_{T_j} \left|\frac{f_{j+1} - f_j}{h}\right|^2 \, dx\right)^{\frac{1}{2}} \\
&\leqslant \frac{\sqrt{|\Omega|}}{h} \max_{j=1,\ldots,m-1} |f_{j+1} - f_j| \\
&\leqslant \frac{2}{h} \sqrt{|\Omega|} \max\{|f_1|, |f_m|, \|F\|_\infty\}. \qquad \square
\end{aligned}$$

In the following we denote the i-th component of $\vartheta(y_n)$ by $\vartheta(y_n)_i$ and we get

$$\begin{aligned}
&\left\|n_h(\cdot, t_l) - \vartheta(y_l)_6\right\|_{2,\Omega} \\
&\quad \leqslant \sqrt{|\Omega|} \max\{\underbrace{|n_h(x_1, t_l) - n_1|}_{=0}, \underbrace{|n_h(x_m, t_l) - n_m|}_{=0}, \|N(t_l) - N_l\|_\infty\} \\
&\quad = \sqrt{|\Omega|} \|N(t_l) - N_l\|_\infty
\end{aligned}$$

and analogously

$$\left\|p_h(\cdot, t_l) - \vartheta(y_l)_7\right\|_{2,\Omega} \leqslant \sqrt{|\Omega|} \|P(t_l) - P_l\|_\infty.$$

Furthermore we get

$$\begin{aligned}
&\left\|\psi_h(\cdot, t_l) - \vartheta(y_l)_5\right\|_{1,2,\Omega} \\
&\quad \leqslant \left\|\psi_h(\cdot, t_l) - \vartheta(y_l)_5\right\|_{2,\Omega} + \left\|(\psi_h(\cdot, t_l) - \vartheta(y_l)_5)'\right\|_{2,\Omega} \\
&\quad \leqslant \sqrt{|\Omega|} \left(1 + \frac{2}{h}\right) \max\left\{\|\Psi(t_l) - \Psi_l\|_\infty, \frac{\|A_S^T\|}{U_T} \|e(t_l) - e_l\|_\infty\right\}
\end{aligned}$$

if we plug in the boundary conditions. For the other components nothing special needs to be done and we get:

Theorem 6.7 *(Estimate for the coupled system). Let h and τ be the stepsizes in space and time respectively. Let Assumptions 6.3, 3.1, 4.1, 6.1, 6.4 and 5.2 be valid. The semiconductor nodes are connected by a capacitive path and the network contains neither LI-cutsets nor CV-loops with at least one voltage source. Let $A_S^T e$ and h be sufficiently small. Then we have for the solution $w(t_l) \in H$ of the coupled system (7) and the solution y_l of the time discretized system (17) in $t_l \in \mathcal{I}$:*

$$\left\|w(t_l) - \vartheta(y_l)\right\|_H \leqslant M\left(h + h^2 \ln\frac{1}{h}\right) + c_1 \tau^K + c_2 \frac{\tau^K}{h} \quad \text{for } M, c_1, c_2 > 0.$$
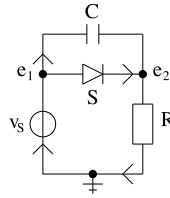
Fig. 1. A simple circuit with a diode and a capacitance in parallel.

Proof. The space discretized system (12) has index one by Theorem 4.2. Hence we can use Theorem 5.1 and the estimates above and get for the second term in (19):

$$\begin{aligned}
\left\| w_h(t_l) - \vartheta(y_l) \right\|_H &\leqslant \left\| e(t_l) - e_l \right\|_\infty + \left\| j_L(t_l) - j_{L,l} \right\|_\infty + \left\| j_V(t_l) - j_{V,l} \right\|_\infty \\
&\quad + \left| j_{S,h}(t_l) - j_{S,h,l} \right| + \left\| \psi_h(\cdot, t_l) - \vartheta(y_l)_5 \right\|_{1,2,\Omega} \\
&\quad + \left\| n_h(\cdot, t_l) - \vartheta(y_l)_6 \right\|_{2,\Omega} + \left\| p_h(\cdot, t_l) - \vartheta(y_l)_7 \right\|_{2,\Omega} \\
&\leqslant \tilde{c}_1 \left\| y(t_l) - y_l \right\|_\infty + \frac{\tilde{c}_2}{h} \left\| y(t_l) - y_l \right\|_\infty, \quad \text{for } \tilde{c}_1, \tilde{c}_2 > 0 \\
&\leqslant c_1 \tau^K + c_2 \frac{\tau^K}{h}, \quad \text{for } c_1, c_2 > 0.
\end{aligned}$$

Using Theorem 6.5 for the first term in (19) gives the desired result. □

The constants c_1, c_2 do not depend on the spatial or temporal stepsize, cf. [9]. The factor M is independent of time by Assumption 6.4 and also does not dependent of the spatial stepsize h because we assumed h to be sufficiently small in Assumption 6.3.

As we can see from Theorem 6.7 we have a restriction on the choice of the time stepsize τ in order to guarantee convergence in the H-norm. We have to make sure that $\tau^K \leqslant h^\alpha$ for an $\alpha > 1$. Since the stepsize h needs to be sufficiently small to guarantee the estimates (21)–(24) this is a restriction on τ.

If we use the L^2-norm for ψ instead of the H^1-norm as before we can define a different norm on H:

$$\begin{aligned}
\left\| w(t) \right\|_H^* &:= \left\| e(t) \right\|_\infty + \left\| j_L(t) \right\|_\infty + \left\| j_V(t) \right\|_\infty + \left| j_S(t) \right| \\
&\quad + \left\| \psi(\cdot, t) \right\|_{2,\Omega} + \left\| n(\cdot, t) \right\|_{2,\Omega} + \left\| p(\cdot, t) \right\|_{2,\Omega}.
\end{aligned}$$

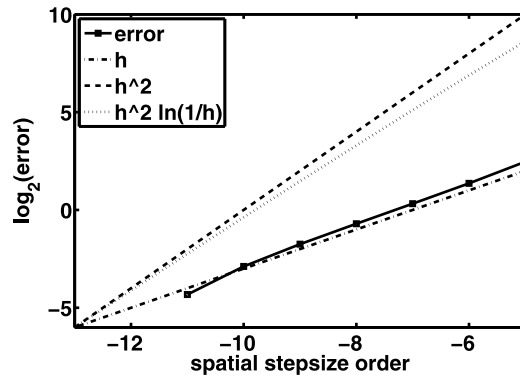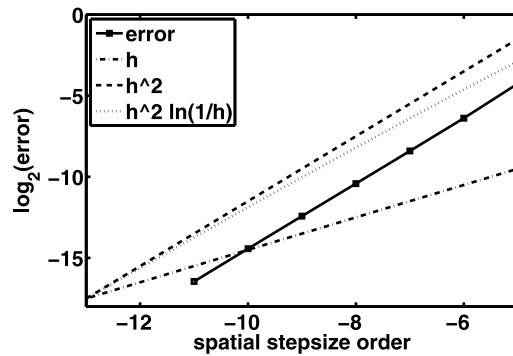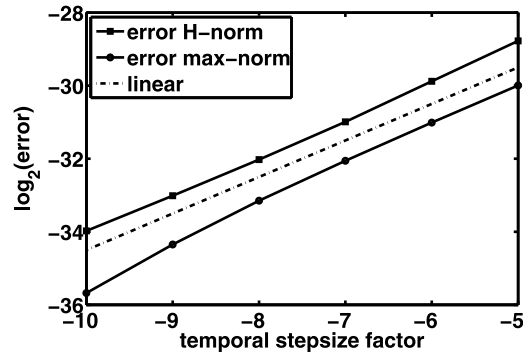Following the same line of argument as above with this norm we get under the same assumptions

$$\left\| w(t_l) - \vartheta(y_l) \right\|_H^* \leqslant M\left(h^2 + h^2 \ln \frac{1}{h} \right) + c_1 \tau^K \quad \text{for } M, c_1 > 0.$$

In this norm we have convergence without restrictions on the time stepsize τ related to the space discretization. However it is a weaker norm in the sense that it is not measuring the error in the derivative of ψ which is the electrical field $E = -\psi'$. We emphasize that the results above have been proven for small applied potentials.

7. Numerical experiments

The convergence result we achieved in Theorem 6.7 can be verified by numerical computations. The estimates which were done for the DD-model itself and index-one DAEs are already well discussed and investigated in the literature, cf. [12, 9,23]. However it is interesting to see that the DD-estimates are also visible when looking at the coupled problem. Therefore we take a simple circuit with a diode, a linear resistance of 10 Ω and a sinusoidal voltage source with amplitude 1 V and frequency 1 kHz, cf. Fig. 1. A parallel small linear capacitance of 10^{-16}F is added to the circuit to fulfill the topological index one conditions of Theorem 4.2. This system was solved with the circuit simulator MECS [7]. We splitted the spatial interval of the diode into 2^5 up to 2^{10} subintervals and compared the numerical solutions to a reference solution which we obtained by using an even finer grid. The result at time point $t = 10^{-5}$ can be seen in Fig. 2 where we see the dominating $\mathcal{O}(h)$ behavior in the H-norm. Evaluating at different time points shows the same behavior. For time integration we used a BDF solver with adaptive stepsize and order control, compare [8]. So the errors with respect to τ are expected to be sufficiently small. We also measured the error in the H^*-norm, cf. Fig. 3. We see here $\mathcal{O}(h^2)$ behavior which is better than the $\mathcal{O}(h^2 \ln \frac{1}{h})$ behavior as expected in theory. Further investigations with different examples are needed here.

In order to observe the temporal estimate we used an implicit Euler scheme (BDF for $K = 1$) with constant temporal stepsize. Therefore we splitted the timeinterval $[0, 10^{-4}]$ into 2^5 up to 2^{10} subintervals and computed a numerical solution for a fixed spatial grid. The error in comparison to a reference solution is plotted in Fig. 4 where we see the expected linear

Fig. 2. Convergence order in H-norm w.r.t. the spatial stepsize h.

Fig. 3. Convergence order in H^*-norm w.r.t. the spatial stepsize h.

Fig. 4. Convergence order in the $\| \cdot \|_\infty$- and the H^*-norm w.r.t. the temporal stepsize τ.

convergence order. The dependency of τ on h does not seem to be a problem here since simulations with different stepsizes show the same magnitude in the error as shown in Fig. 4. Reducing the spatial stepsize even more led to problems in the convergence of the Newton solver which might be caused by the $\mathcal{O}(\frac{\tau^K}{h})$ term.

8. Conclusions

In this paper we investigated a PDAE system which arises when coupling the MNA circuit equations to the stationary one-dimensional DD-model. We proved an index one result where the existence of a capacitive path between the semiconductor nodes is a mathematically crucial condition which is also physically motivated. Relying on existing convergence estimates for the DD-model and DAEs we showed a convergence estimate for the whole coupled system. These estimates were also observed numerically.

A generalization of the presented results to the two or three-dimensional DD-model seems to be possible. The existence of a solution of the coupled system in the multidimensional case is given in [2]. The spatial discretization of the DD-model is also described in [12]. However special care has to be taken of the boundary conditions for the drift diffusion equations

because they describe the coupling to the circuit equations. A detailed description can be found in [22]. Furthermore the assumptions underlying the classical estimates (21)–(24) get more severe especially concerning the geometry, cf. [12]. The assumption that the involved fast varying quantities have to be resolved sufficiently well by the mesh will have even more impact on numerical solutions than in the one-dimensional case. It is well known in the multidimensional case that for reasonable numerical results an adaptive spatial grid is needed for the DD-part, cf. [20,12].

Other spatial discretization schemes seem to be possible as well. However it has to be ensured that the corresponding operator G'_{DD} is invertible in order to obtain the index one result in Theorem 4.2. Furthermore convergence estimates like (21)–(24) are needed to produce an analogous result to Theorem 6.7. A description of various finite element discretization methods for semiconductor devices can be found in [15].

References

[1] G. Alì, A. Bartel, M. Günther, C. Tischendorf, Elliptic partial differential-algebraic multiphysics models in electrical network design, Math. Models Methods Appl. Sci. 13 (9) (2003) 1261–1278.

[2] G. Alì, N. Rotundo, An existence result for elliptic partial differential-algebraic equations arising in semiconductor modeling, Nonlinear Anal. Theory Methods Appl. 72 (12) (2010) 4666–4681.

[3] M. Bodestedt, Perturbation analysis of refined models in circuit simulation, Ph.D. thesis, Technical University of Berlin, 2007, http://opus.kobv.de/tuberlin/volltexte/2008/1713/.

[4] L.O. Chua, C.A. Desoer, E.S. Kuh, Linear and Nonlinear Circuits, McGraw-Hill Book Co., Singapore, 1987.

[5] H. Gajewski, K. Gröger, On the basic equations for carrier transport in semiconductors, J. Math. Anal. Appl. 113 (1986) 12–35.

[6] C.W. Gear, Numerical Initial Value Problems in Ordinary, Differential Equations, Prentice Hall PTR, New York, 1971.

[7] C. Guhlke, M. Selva, MECS manual, http://www.mi.uni-koeln.de/~mselva/MECS.html, 2007.

[8] M. Hanke, A new implementation of a BDF method within the method of lines, Report No. 2001:01, Royal Institute of Technology, Stockholm, 2001.

[9] I. Higueras, R. März, Differential-algebraic equations with properly stated leading terms, Comput. Math. Appl. 48 (2004) 215–235.

[10] C. Ho, A. Ruehli, P. Brennan, The modified nodal approach to network analysis, IEEE Trans. Circuits Syst. 22 (6) (1975) 504–509.

[11] A. Jüngel, Mathematical modeling of semiconductor devices, University Konstanz, http://asc.tuwien.ac.at/~juengel/scripts/semicond.pdf, 2002.

[12] P.A. Markowich, The Stationary Semiconductor Devices, Springer, Vienna, 1986.

[13] R. März, Nonlinear differential-algebraic equations with properly formulated leading term, Tech. Rep. 3, Institute of Mathematics, Humboldt-University of Berlin, 2001.

[14] M. Matthes, Konvergenzanalyse einer gekoppelten Schaltungs- und Bauelementsimulation, Master's thesis, University of Cologne, http://www.mi.uni-koeln.de/~mmatthes/Diplomarbeit_MMatthes.pdf 2008.

[15] J.J.H. Miller, W.H.A. Schilders, S. Wang, Application of finite element methods to the simulation of semiconductor devices, Rep. Prog. Phys. 62 (1999) 277–353.

[16] M.S. Mock, Analysis of Mathematical Models of Semiconductor Devices, Boole-Press, Dublin, 1983.

[17] R.M. Pringle, A.A. Rayner, Generalized Inverse Matrices, Griffin, London, 1971.

[18] D. Scharfetter, H. Gummel, Large signal analysis of a silicon read diode oscillator, IEEE Trans. Electron Devices 16 (1969) 66–77.

[19] D.E. Schwarz, C. Tischendorf, Structural analysis of electrical circuits and consequences for MNA, Int. J. Circuit Theory Appl. 28 (2000) 131–162.

[20] S. Selberherr, Analysis and Simulation of Semiconductor Devices, Springer, Vienna, 1984.

[21] M. Selva, C. Tischendorf, Numerical analysis of DAEs from coupled circuit and semiconductor simulation, Appl. Numer. Math. 53 (2–4) (2005) 471–488.

[22] C. Tischendorf, Coupled systems of differential algebraic and partial differential equations in circuit and device simulation, Habilitationsschrift, Humboldt University of Berlin, http://www.mi.uni-koeln.de/~ctischen/publications.html 2004.

[23] S. Voigtmann, General linear methods for integrated circuit design, Ph.D. thesis, Humboldt University of Berlin, 2006, http://nbn-resolving.de/urn:nbn:de:kobv:11-10069614.